

Unsupervised Domain Adaptation for Device-free Gesture Recognition

Bin-Bin Zhang, Dongheng Zhang, Yadong Li, Yang Hu, and Yan Chen, *Senior Member, IEEE*

Abstract—Device-free human gesture recognition with Radio Frequency (RF) signals has attained acclaim due to the omnipresence, privacy protection, and broad coverage nature of RF signals. However, neural network models trained for recognition with data collected from a specific domain suffer from significant performance degradation when applied to a new domain. To tackle this challenge, we propose an unsupervised domain adaptation framework for RF-based gesture recognition by making effective use of the unlabeled target domain data. Specifically, we apply pseudo-labeling and consistency regularization with elaborated design on target domain data to produce pseudo-label and align instance’s feature of the target domain. Then, we design two data augmentation methods by randomly erasing the input data to enhance the robustness of the model. Furthermore, we apply a confidence control constraint to tackle the overconfidence problem. We conduct extensive experiments on a public Wi-Fi dataset and a public millimeter wave (mmWave) radar dataset. The experimental results demonstrate the superior effectiveness of the proposed framework.

Index Terms—Gesture Recognition, Cross Domain, Unsupervised Domain Adaptation, Device Free.



1 INTRODUCTION

HUMAN gesture recognition plays an important role in human-computer interaction, enabling applications including smart home, smart driving and virtual reality, etc. Traditional approaches adopt cameras [1], [2], wearable devices and phones [3], [4] as the sensing module, which however suffer from inherent drawbacks including privacy leakage, inconvenience, and limited sensing range. To address this challenge, significant efforts [5]–[19] have recently been made to explore Radio Frequency (RF)-based human gesture recognition techniques without letting the monitored subject carry a dedicated device. These techniques recognize gestures by perceiving RF signals variations caused by gestures in space. However, the signals arriving at the receiver not only contain information of the performed gestures, but also carry substantial information of the environment, subject, location, and orientation. We usually use the term “domain” to summarize these gesture irrelevant factors. As a result, the classifiers trained with data in one domain usually undergo drastically performance drop in another domain.

To tackle this problem, researchers have explored how to improve cross domain RF-based device-free gesture recognition performance. These RF-based methods can be roughly divided into two categories: Wi-Fi-based and mmWave-based methods. Among the Wi-Fi-based methods, WiAG [20] and Widar3.0 [21] construct mathematical models to derive features that are independent of users’ location and orientation. However, WiAG doesn’t consider cases across environments and subjects, Widar3.0 still can not remove all

the influence of domain. CrossSense [22] proposes an offline trained ANN-based roaming model mapping features from one environment to another, which however is not applicable to the case with multiple source domains. Then EI [23] and CACDGR [24] are proposed by using an adversarial training to improve the cross domain performance of recognition model. However, EI [23] doesn’t consider location and orientation’s influence, CACDGR [24] needs an amount of extra training efforts. Though the above methods improve the performance of the recognition models, they need extra neural network modules and an amount of extra training efforts. For the mmWave-based methods, Liu et al. [25] extract dynamic variation of gestures from mmWave signals and design a lightweight CNN to recognize gestures. MmASL [26] designs a multi-task deep neural network to achieve American sign language recognition. RadarNet [27] designs an efficient neural network and collects a large scale dataset to train a robust model. However, for cross domain situation, these mmWave-based recognition models can not perform as well as the in-domain situation.

Due to the fact that the signal propagation in practical environment is very complicated, the data distributions collected from different domains may be very different. Thus, the model trained with source domain data cannot be directly generated to unlabeled target domain. To tackle this challenge, a common solution is to collect labeled target domain data and transfer the trained model into target domain. However, such data collection is costly and not practical in deployment. Compared with labeled data, unlabeled data is more accessible which also contains the information of the target domain.

In this paper, we propose an unsupervised domain adaptation framework for FR-based device-free gesture recognition to increase the recognition model’s ability of cross-domain. Inspired by the semi-supervised learning (SSL) techniques [28]–[33], we propose the pseudo-labeling technique and consistency regularization strategy

- B. Zhang, D. Zhang, Y. Li, Y. Chen are with the School of Cyber Science and Technology, University of Science and Technology of China, Hefei 230026, China.
(E-mail: robin18@mail.ustc.edu.cn, dongheng@ustc.edu.cn, yadongli@mail.ustc.edu.cn, eecyan@ustc.edu.cn).
- Y. Hu is with the School of Information Science and Technology, University of Science and Technology of China, Hefei 230026, China.
(E-mail: eeyhu@ustc.edu.cn).

with elaborated design on target domain data to make effective use of the unlabeled target domain data. Among the two techniques, pseudo-labeling can produce labels for unlabeled target data which can further be utilized to train recognition model. With the aid of pseudo label, the generalization ability of the model could be enhanced. Consistency regularization would align instance’s feature of the target domain data by decreasing the gap between original feature and augmented version of original feature, which can make the model pay more attention to the intrinsic feature associated with gesture category. More importantly, we combine these two techniques with elaborated design rather than employing them independently, which make the training process simple and efficient. Specifically, the pseudo labels produced based on unlabeled target domain data are adopted as targets of augmented version of the same data. In addition, we propose two data augmentation methods for RF signals by randomly erasing the feature of input data, which can enhance the effectiveness of the consistency regularization. And we adopt a confidence control constraint to tackle the overconfidence problem, which would lead to the model predicting wrong high confident classification.

Our main contributions are summarized as follows:

- We propose an unsupervised domain adaptation framework for RF-based device-free gesture recognition to improve cross domain performance of the neural network.
- We propose the pseudo-labeling and consistency regularization techniques with elaborated design to make effective use of the unlabeled RF data in target domain. In addition, we design a confidence control constraint to tackle the overconfidence problem. According to the characteristics of RF signals, we design two data augmentation methods to enhance the effectiveness of the consistency regularization.
- We conduct comprehensive experiments on a public Wi-Fi dataset and a public mmWave radar dataset. Our framework achieves better performance than state-of-the-art models, which demonstrates the superiority and generalization ability of our framework.

The rest of this paper is organized as follows. Section 2 introduces the related work. Section 3 formulates the problem. Section 4 introduces the system overview, recognition model and the proposed unsupervised domain adaptation framework. Section 5 presents the experiments on the two RF-based signals, the performance of the cross domain evaluations and the ablation study. Section 6 concludes this paper.

2 RELATED WORK

Inspired by the semi-supervised learning (SSL) techniques, we propose an unsupervised domain adaptation framework for device-free gesture recognition. The proposed framework is related to these three techniques: *unsupervised domain adaptation*, *semi-supervised learning* and *cross domain gesture recognition*.

2.1 Unsupervised Domain Adaptation

The UDA models assume that the source domain has sufficient labels, while the unlabeled target domain participates the model training in an unsupervised manner [34]. Several approaches are adopted to learn domain-invariant features through different metrics, e.g., Maximum Mean Discrepancy (MMD) [35], [36]. Contrastive Adaptation Network (CAN) [37] optimizes the metric for minimizing the domain discrepancy, which explicitly models the intra-class domain discrepancy and the inter-class domain discrepancy. Deep Adaption Network (DAN) [35] adapts the high-layer features with the multi-kernel MMD criterion. Adversarial discriminative domain adaptation (ADDA) [38] learns a discriminative representation using the source labels, and then, a separate encoding that maps the target data to the same space based on a domain-adversarial loss is used. General to Adapt (GTA) [39] introduces a symbiotic relation between the embedding network and the generative adversarial network. Some other methods aim to learn a feature extractor to extract the domain-invariant features, and maintain the representation consistency through minimizing the reconstruction error between domains. For example, Domain Adversarial Neural Network (DANN) [40] proposes a domain-adversarial training method to promote the emergence of features that are discriminative for the main learning task on the source domain. Unsupervised Image-to-Image Translation (UNIT) [41] makes a shared-latent space assumption and proposes an unsupervised image-to-image translation framework based on Coupled GANs. Different from the existing UDA methods, our framework adopts the pseudo-labeling and consistency regularization on target domain to obtain pseudo labels and align instance’s feature of the target domain data, which can make effective use of the unlabeled target domain data.

2.2 Semi-Supervised Learning

Semi-supervised learning (SSL) [29], [31], [33], [42]–[44] leverages unlabeled data to improve a model’s performance when limited labeled data is provided, which alleviates the expensive labeling process efficiently. Some recently proposed semi-supervised learning methods, such as MixMatch [43], FixMatch [31], and ReMixMatch [42], are based on augmentation viewpoints. MixMatch [43] uses low-entropy labels for data-augmented unlabeled instances and mixes labeled and unlabeled data for semi-supervised learning. FixMatch [31] generates pseudo labels using the model’s predictions on weakly augmented unlabeled images. ReMixMatch [42] uses a weakly-augmented example to generate an artificial label and enforce consistency against strongly-augmented examples. Semi-supervised domain adaptation has more information about some target labels compared with UDA, and some related works [45]–[49] have been proposed leveraging semi-supervised signals. Specifically, in [46], a minimax entropy approach is proposed that adversarially optimizes an adaptive few-shot model. In [47], the learning of opposite structures is unified whereby it consists of a generator and two classifiers trained with opposite forms of losses for a unified object. Inspired by the semi-supervised learning (SSL) techniques, we propose an UDA framework for RF-based gesture recognition. Specially, we

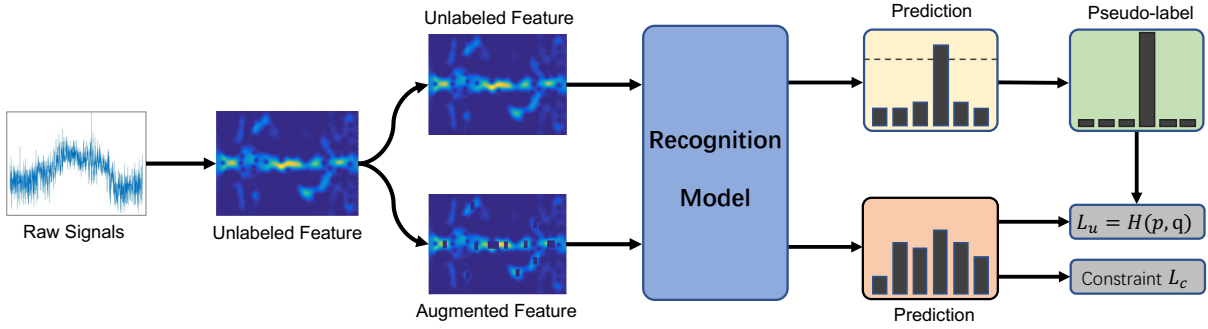


Fig. 1: Overview of our framework. After an unlabeled original feature being fed into the model, we obtain the predictions. When the model assigns a probability to any class which is above a threshold, we obtain pseudo-label. Then we obtain the model’s predictions for augmentation version of the same feature. We train the model by computing and optimizing the cross-entropy loss between prediction on the augmented version and the pseudo-label.

combine the pseudo-labeling and consistency regularization with elaborated design and use the model’s predictions on original unlabeled samples to obtain the pseudo labels.

2.3 Cross Domain Gesture Recognition

Wireless human sensing techniques [50]–[55] have drawn considerable attention and made great progress in recent years. Due to the fact that human gesture recognition is a core part of human-computer interaction, researchers explore how to improve the performance of the RF-based gesture recognition. There are many prior works focusing on cross domain gesture recognition to reduce data collection and labeling efforts to generalize the recognition model, which can be roughly divided into two categories: Wi-Fi-based and mmWave-based methods.

Among the Wi-Fi-based methods, WiAG [20] and Widar3.0 [21] construct mathematical models to derive features that are independent of users’ location and orientation. CrossSense [22] proposes an offline trained ANN-based roaming model mapping features from one environment to another. EI [23] uses an adversarial training scheme together with several constraints to generalize the model to new environments and new subjects. WiHARAN [56] aligns the joint distributions of features and activity classes of samples from multiple domains by adversarial learning. CACDGR [24] presents a model using an adversarial learning scheme together with feature disentanglement modules that can remove the influence of the domain. Though the above methods improve the performance of the recognition model, they need an amount of extra training efforts. For the mmWave-based models, Liu et al. [25] extract dynamic variation of gestures from mmWave signals and design a lightweight CNN to recognize gestures. MmASL [26] designs a multi-task deep neural network to achieve American sign language recognition. RadarNet [27] designs an efficient neural network and collects a large scale dataset to train a robust model. However, for cross domain situation, these mmWave-based recognition models can not perform as well as the in-domain situation. In this paper, we introduce an unsupervised domain adaptation framework for device-free gesture recognition adopting the pseudo-labeling and consistency regularization with elaborated design.

3 PROBLEM FORMULATION

The input data contains both labeled and unlabeled ones. We refer to the data with and without gesture labels as source and target domain, respectively. All the data are attached with domain labels including four dimensions, i.e., environment, subject, location and orientation, indicating under what configurations the data are collected. Suppose there are N source domains corresponding to N different underlying distributions $\{p_{s_i}(x, y)\}_{i=1}^N$. Source domains’ data are sampled from N distributions respectively with gesture labels, denoted as $(X_{s_i}, Y_{s_i}) = \{x_{s_i}^j, y_{s_i}^j\}_{j=1}^{n_{s_i}}$, where $i \in \{1, \dots, N\}$. We regard the target domain as a whole set without label, denoted as $X_t = \{x_t^j\}_{j=1}^{n_t}$. All the source domains and target domain have the same gesture categories. In this paper, we aim to improve the performance of the recognition model trained using labeled source domain data and unlabeled target domain data on target domain.

4 METHODOLOGY

In this section, we present our unsupervised domain adaptation framework for RF-based gesture recognition. First, we provide an overview of our framework. Next, we introduce the input of the recognition model. Then, we illustrate each module of the unsupervised domain adaptation framework. Finally, we give the objective function and training strategy.

4.1 Overview

An overview of the proposed framework is shown in Fig. 1. The framework aims to train a gesture recognition model using the unlabeled target data and labeled source domain data. Since the collected gesture data contain temporal information and exist multiple links, the recognition model can be built up by CNN and GRUs to extract discriminative features and classify the gesture categories. To mitigate domain discrepancies between target and each source domain, we adopt the two techniques: pseudo-labeling and consistency regularization in our framework. Pseudo-labeling produces pseudo labels of unlabeled target data which can be utilized to increase the generalization ability of the recognition model. Consistency regularization strategy can align instance’s feature of the target domain data, which

can make the model pay more attention to the intrinsic feature associated with gesture category. We combine these two techniques with elaborated design rather than employing them independently, which make the training process simple and efficient. In addition, we propose two data augmentation methods for RF signals by randomly erasing the feature of input data, which can enhance the effectiveness of the consistency regularization. And we adopt a confidence control constraint to tackle the overconfidence problem, which would lead to the model predicting wrong high confident classification. The details of our framework will be elaborated in the rest of this section.

4.2 Model Inputs

Our framework can be used for different RF signals. In this paper, we consider two types of RF signals: Wi-Fi signal and mmWave radar signal. We choose the Body-coordinate Velocity Profile (BVP) feature and Dynamic Range Angle Image (DRAI) sequences as the input of our model, respectively. BVP feature is obtained by body-coordinate velocity profile generation technique in Widar 3.0 [21]. It describes power distribution over different velocities, at which body parts involved in the gesture movements. BVP feature is a matrix with dimension as $N \times N \times T$, where N is the number of possible values of velocity components decomposed, T is the number of BVP snapshots. mmWave radar signal can be processed to DRAI sequences in [57] to obtain doppler power distribution over spatial positions while reducing environmental noise and multi-path effects. DRAI sequences is a matrix with dimension as $M \times M \times T$, where M is the number of possible values of range and angle, and T denotes the time dimension.

4.3 Recognition Model

As shown in Fig. 2, our model consists of two network components, which are feature extractor and gesture recognizer.

Feature Extractor: We employ one common extractor G to extract gesture features from all the source domains and target domain. We expect that the extractor G can extract the features which are related to gestures. In the feature extractor, we use single-layer CNN with 2D kernels to extract features. After applying a max-pooling layer to down-sample the features and a dropout layer to reduce overfitting, we flatten the 2D features into a feature vector. Then the vector is fed into two dense layers with Relu activation to get a higher level representation \mathbf{U}_t . To extract temporal relationships within feature series, $\mathbf{U} = \{\mathbf{U}_t, t = 1, 2, \dots, T\}$ are fed into single-layer GRUs to generate the feature vector \mathbf{Z} . Given the input series \mathbf{X} , we can obtain feature vector \mathbf{Z} as follows:

$$\mathbf{Z} = G(\mathbf{X}; \Theta). \quad (1)$$

Gesture Recognizer: Based on feature vector \mathbf{Z} , a dropout layer and a dense layer with Relu activation are adopted to learn the representation \mathbf{H}_i as follows:

$$\mathbf{H}_i = \text{Softplus}(\mathbf{W}_z \mathbf{Z}_i + \mathbf{b}_z), \quad (2)$$

where \mathbf{W}_z and \mathbf{b}_z are the parameters to be learned, the softplus function is an activation function. Then a softmax layer is used to obtain the probability vector $\hat{\mathbf{y}}$. For the

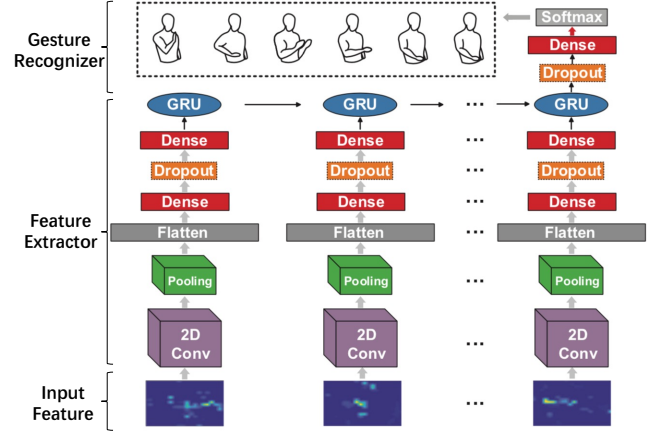


Fig. 2: Structure of gesture recognition module.

labeled source domain data, cross-entropy function is used to calculate the loss between the predictions and the ground truths as follows:

$$L_a = -\frac{1}{|\mathbf{X}^l|} \sum_{i=1}^{|\mathbf{X}^l|} \sum_{c=1}^C \mathbf{y}_{ic}^l \log(\hat{\mathbf{y}}_{ic}^l), \quad (3)$$

where $|\mathbf{X}^l|$ is the number of labeled data, C is the number of categories of human gestures. By optimizing Eq. (3), we can learn model parameters and make predictions on target domain data.

4.4 Unsupervised Domain Adaptation Framework

To improve the cross domain generalization ability of the recognition model, we propose an unsupervised domain adaptation framework for the RF-based gesture recognition. As shown in Fig. 1, we propose the two techniques: *pseudo-labeling* and *consistency regularization* with elaborated design to make effective use of the unlabeled target domain data.

We first obtain μB unlabeled data \mathbf{X}^u from target domain data pool X_t , where B is a batch of labeled data and μ is a hyperparameter that determines the relative sizes of B and μB . Then we augment \mathbf{X}^u with two kinds of data augmentation strategies, which is denoted by $\mathcal{A}(\cdot)$. After that, we concatenate the source domain labeled data \mathbf{X}^l , unlabeled target domain data \mathbf{X}^u , and augmented version data \mathbf{X}_{aug}^u as follows:

$$\begin{aligned} \mathbf{X}_{aug}^u &= \mathcal{A}(\mathbf{X}^u), \\ \mathbf{X}_{in} &= \mathbf{X}^l + \mathbf{X}^u + \mathbf{X}_{aug}^u. \end{aligned} \quad (4)$$

When we input the \mathbf{X}_{in} into the model, the output can be obtained by $\hat{\mathbf{y}} = [\hat{\mathbf{y}}^l, \hat{\mathbf{y}}^u, \hat{\mathbf{y}}_{aug}^u]$, where $\hat{\mathbf{y}}^u$ denotes the predictions of unlabeled data, $\hat{\mathbf{y}}_{aug}^u$ denotes the predictions of augmented version.

4.4.1 Pseudo-Labeling

Making effective use of the target domain data can enhance the recognition model's ability of domain adaptation. Due to the fact that the target domain data have no labels, we propose to utilize the pseudo-labeling technique to make effective use of the unlabeled target domain data. Pseudo-labeling technique can produce pseudo labels of unlabeled

target data that are used to train recognition model. Training the model with target data can increase the ability of adaptation on target domain. During training, right pseudo labels can speed up the convergence of the model and improve the performance of the model, while the incorrect one will cause the negative impact on the training of model [33]. To address this problem, we expect to obtain the "hard" labels. In specific, when the largest class probability of $\hat{\mathbf{y}}^u$ surpasses the threshold τ , the pseudo label \mathbf{y}^u can be obtained as follows:

$$\mathbf{y}_{ij}^u = \begin{cases} 1, & \hat{\mathbf{y}}_{ij}^u \geq \tau, \\ 0, & \text{otherwise.} \end{cases} \quad j = 1, 2, \dots, C \text{ and } i = 1, 2, \dots, |X^u|, \quad (5)$$

where $|X^u|$ is the number of the unlabeled data. With model training, the confidence of output also increases. In order to ensure the effectiveness of the pseudo labels, we use the dynamic threshold, which increases with the number of iterations as follows:

$$\tau_d = \tau_0 + \eta \text{ epoch} \quad (6)$$

where τ_d is the dynamic threshold, τ_0 is the initial value of threshold, η denotes the updated step size and *epoch* is the number of iterations.

After obtaining pseudo labels of unlabeled examples, we add the data with pseudo labels to the training set. Different from the other traditional methods, we adopt the pseudo labels as the target of the augmented version of the unlabeled data \mathbf{X}_{aug}^u rather than \mathbf{X}^u to combine the pseudo-labeling technique and consistency regularization with elaborated design, which can make our framework simple and effective.

4.4.2 Consistency Regularization

Consistency regularization is an important component of recent state-of-the-art SSL algorithms [29], [29], [32]. Inspired by SSL algorithms, we propose to utilize consistency regularization to align instance's feature of the target domain data by decreasing the gap between original feature and augmented version of original feature, which can force the recognition model to learn the essential characteristics of gestures, which can weaken the influence of the domain. Specifically, we expect the model to output similar predictions when fed different versions of the same data. We first augment the unlabeled target domain data to gain the version of the target domain data. Once the original data and the augmented data have been fed into the recognition model, we obtain the two predictions of unlabeled data $\hat{\mathbf{y}}^u$ and the predictions of augmented version $\hat{\mathbf{y}}_{aug}^u$. Then we measure the discrepancies between the predictions of unlabeled data $\hat{\mathbf{y}}^u$ and the predictions of augmented version $\hat{\mathbf{y}}_{aug}^u$.

After obtaining the predicted probabilities of unlabeled data $\hat{\mathbf{y}}^u$ and the predicted probabilities of augmented same unlabeled data $\hat{\mathbf{y}}_{aug}^u$, we expect the two predictions be similar as much as possible so that they belong to the same classification category. That is equivalent to the two predictions can produce the same pseudo labels. To achieve this goal, we train the recognition model by adopting the pseudo label \mathbf{y}^u as target of $\hat{\mathbf{y}}_{aug}^u$, computing and reducing

the cross-entropy loss between the target \mathbf{y}^u and $\hat{\mathbf{y}}_{aug}^u$. The loss function L_u can be defined as follow:

$$L_u = -\frac{1}{|\mathbf{y}^u|} \sum_{i=1}^{|\mathbf{y}^u|} \sum_{c=1}^C \mathbf{y}_{ic}^u \log(\hat{\mathbf{y}}_{aug\ ic}^u), \quad (7)$$

where $|\mathbf{y}^u|$ is the number of pseudo labels. The goal of unsupervised domain adaptation framework is to minimize the loss L_u .

4.4.3 Confidence Control Constraint

In our framework, whether it can be beneficial to our framework or not mainly depends on the accuracy of the pseudo-labeling. The right pseudo labels can speed the convergence of the model up and improve the performance of the model, but the incorrect pseudo labels will cause the negative impact on the training of model. As the model with only source domain data for training is prone to overfitting on the target domain data, the predictions on target domain $\hat{\mathbf{y}}^u$ tend to be overconfident on incorrect categories and produce incorrect pseudo labels. Such phenomenon will make the model undergo drastically drop in accuracy. To tackle this problem, we expect the probability distribution $\hat{\mathbf{y}}^u$ not too overconfident. So we adopt an effective constraint L_c to achieve this goal. In specific, we compute and reduce the cross-entropy loss between the predictions of unlabeled data $\hat{\mathbf{y}}^u$ and the vector \mathbf{I} , where \mathbf{I} is a vector whose every element equals to one. The loss is defined as follows:

$$L_c = -\frac{1}{|\mathbf{y}^u|} \sum_{i=1}^{|\mathbf{y}^u|} \sum_{c=1}^C \log(\hat{\mathbf{y}}_{ic}^u). \quad (8)$$

In particular, the loss is equivalent to Kullback–Leibler (KL) divergence between the predictions of unlabeled data $\hat{\mathbf{y}}^u$ and the vector \mathbf{I} , which measures the discrepancy between the vector \mathbf{I} and the unlabeled target probabilities $\hat{\mathbf{y}}^u$. Reducing the loss can make the $\hat{\mathbf{y}}^u$ be similar to the vector \mathbf{I} so that the $\hat{\mathbf{y}}^u$ is not overconfident.

4.4.4 Data augmentation

Reducing the gap between original feature and augmented version of original features is the key procedure of the consistency regularization. When transforming the original features, we can not change the semantics of the feature. Thus, the augmentation methods for images cannot be directly applied to RF signals (i.e., WiFi signal and mmWave signal). To tackle this challenge, we design two data augmentation methods: *Feature Erasing* and *Time Erasing* as below.

(1) *Feature Erasing*: Due to the fact that the local features contain unique domain information, paying too much attention to the local feature will lead to the performance degradation. To solve the problem, we expect the model pays more attention to the overall feature associated with the gesture category. Inspired by [58], we select some local features randomly and erase them by making their value equal to zero. To ensure that the semantics remain unchanged, we do not focus on erasing a certain area. The details can be described as follows:

$$\mathbb{F}_{(i,j)}^{(t)} = 0, \quad t = 1, 2, \dots, T, \quad (i, j) \in \text{Rand}(m), \quad (9)$$

where $\mathbb{F}^{(t)}$ is the feature of t -th time dimension, whose dimensions are $N \times N$, $\text{Rand}(m)$ denotes local feature

coordinates to be erased and m is the number of erasing feature.

(2) *Time Erasing*: Deep neural networks are prone to overfitting without sufficient data, which usually leads to disappointing performance. Actually, it is usually difficult to collect sufficient gesture data in device-free gesture recognition scenarios. Therefore, increasing the number and diversity of gestures is helpful to boost the model performance. Erasing the feature on time dimension within the certain number can increase the number and diversity of data. Inspired by [59], we augment the data in the time dimension with time erasing, i.e., we choose a certain number of frames of the sample randomly, then make the frames' feature value be zero. This process can be expressed as:

$$\mathbb{F}^{(i)} = 0, i \in \text{Rand}(q), \quad (10)$$

where $\mathbb{F}^{(i)}$ is the feature of i -th time dimension, whose dimensions is $N \times N$, $\text{Rand}(q)$ denotes time dimensions to be erased and q is the number of erasing time feature.

4.5 Objective and Training

The final objective is composed of classification loss, unsupervised domain adaptation loss, and constraint loss. The objective function is defined as follows

$$L = L_a + \lambda L_u + \eta L_c, \quad (11)$$

where L_a is the classification loss, L_u is the unsupervised domain adaptation loss and L_c is the confidence control constraint loss, λ represents the weight of the loss L_u , η is the weight of the loss L_c . In the training process, we iteratively update the parameters according to SGD [60].

5 EXPERIMENTS

In this section, we conduct experiments on two different RF-based gesture recognition testbeds, i.e., Wi-Fi and mmWave, to evaluate the performance of the proposed framework. We also conduct the ablation experiments to analyze the modules in our framework.

5.1 Experiment with Wi-Fi Signals

5.1.1 Dataset

We adopt the public Widar 3.0 [21] dataset. The dataset is collected from 3 rooms, 16 users, 5 locations and 5 orientations in total. Fig. 3(a) shows the layouts and sensing areas of the three experimental environments containing various types, i.e., classroom, hall and office. Fig. 3(b) shows a typical examples of the deployment of devices and domain configurations in the sensing area, which is a $2m \times 2m$ square. In this study, we classify 6 commonly used gestures as shown in Fig. 3(c). The dataset contains 11250 data samples (15 users \times 5 positions \times 5 orientations \times 6 gestures \times 5 instances).

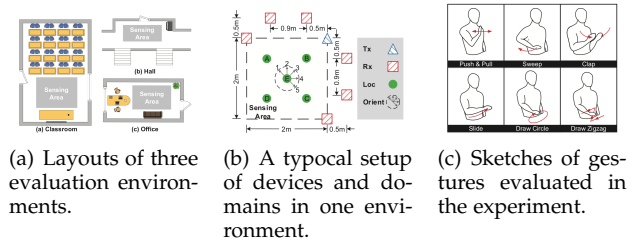


Fig. 3: Experimental setting with Wi-Fi signals, figure from [21].

5.1.2 Data Preprocessing

In our experiments, we use BVP as our model input. BVP is proposed by Widar 3.0 [21] to remove the influence of the domain by describing power distribution over different velocities. With the noises and offsets filtered out, only prominent multipath components with non-zero DFS are retained. Further applying short-term Fourier transform yields power distribution over the time and Doppler frequency domains, the DFS can be obtained. After that, we establish the local body coordinates whose origin is the location of the person and positive x -axis aligns with the orientation of the person. Then we exploit existing passive tracking systems to obtain the location and orientation of the person. All locations and orientations used in the following derivation are in the local body coordinates. Any velocity components around the human body will contribute its signal power to some frequency component. Finally, we adopt the idea of compressed sensing to estimate BVP feature.

5.1.3 Baseline Methods

We compare our approach with three deep learning models CrossSense [22], EI [23] and Widar3.0 [21]. Specifically, CrossSense proposes an ANN-based roaming model to translate signal features from source domains to target domains, and employs multiple expert models for gesture recognition. EI is a state-of-the-art adversarial learning scheme for unsupervised domain adaptation, which can be applied for multiple source domains and target domains. It is composed of one feature extractor, one domain discriminator and one gesture classifier in EI. In Widar 3.0 [21], the authors extract the domain invariant feature BVP based on DFS data and feed them into a model combining CNN's and GRUs.

5.1.4 Cross Domain Evaluation

We evaluate the performance of our framework on cases crossing different domain factors, including orientation, location, subject, and environment. When we evaluate on each domain factor, we keep the other domain factors unchanged. For each case, all of the target domain data without labels are used to train with the source data and all the target domain data are used to test. The numbers or letters behind the arrow \rightarrow represents the target domain data. We conduct experiments using all the baseline methods to validate our framework's superiority.

(1) *Cross Orientation*: In this experiment, we select data of one orientation in all rooms as the target domain and

TABLE 1: Cross Orientation Accuracy (%)

Methods	→ 1	→ 2	→ 3	→ 4	→ 5	Avg
CrossSense	69.41	80.23	80.45	83.18	70.07	76.67
EI	70.42	81.15	88.16	90.83	70.74	80.26
Widar 3.0	80.24	89.64	89.05	82.75	72.64	82.86
Ours	87.44	91.64	91.98	85.46	79.53	87.21

TABLE 2: Cross Location Accuracy (%)

Methods	→ A	→ B	→ C	→ D	→ E	Avg
CrossSense	88.61	85.23	82.89	78.94	85.16	84.16
EI	87.91	90.13	86.85	85.82	93.14	88.77
Widar 3.0	89.14	89.10	90.50	89.50	95.15	90.67
Ours	90.47	90.30	92.30	90.44	95.86	91.87

TABLE 3: Cross Subject Accuracy (%)

Methods	→U10	→U11	→U12	→U13	→U14	→U15	→U16	→U17	Avg
CrossSense	77.67	81.35	80.24	83.73	85.97	82.43	80.19	82.59	81.77
EI	80.11	83.56	85.91	82.05	84.36	85.44	81.23	86.21	83.61
Widar 3.0	86.26	90.13	83.33	89.86	87.73	89.97	91.46	88.34	88.38
Ours	86.79	89.73	80.93	91.60	88.13	92.51	91.33	90.67	88.96

the other 4 orientations as the source domains in the three rooms, 15 Users’s data. Table 1 shows that the proposed method has an overall accuracy of 87.21%, which is the highest average accuracy comparing to other methods. Even in this case, our method has an improvement of 4.35% over Widar 3.0. Orientation 2 and 3 have an accuracy above 90% while the accuracy declines over 10% for orientation 5. This is reasonable since orientation 5 is too faraway and the receiver may not capture the full information of gestures.

(2) *Cross Location*: Similar to the cross orientation settings, to evaluate the performance of crossing location, we use data of 4 locations in all rooms as the source domains, and the data of the last location as the target domain. The result comparison is shown in Table 2. Compared to other methods, our framework achieves the highest average accuracy of 91.87%. Our framework has an accuracy above 90% on all location domains. Location E has the highest accuracy of 95.86%, which is reasonable since location E is the center of other four locations. In addition, the average accuracy of our method is 1.2% higher than Widar 3.0.

(3) *Cross Subject*: Data collected from different persons may have discrepancies due to their various behavior patterns and their body shapes. To evaluate on different subjects, we use data from *User 9 – 17* in Room 1. Each time, we use the data from one user as the target domain and the other users’ data as the source domains. The results in Table 3 show our framework achieves the highest average accuracy of 88.83%. In addition, the average accuracy of our method is 0.58% higher than Widar 3.0.

(4) *Cross Environment*: To evaluate the impact of the environment, we use the gesture samples collected in two

TABLE 4: Cross Environment Accuracy (%)

Methods	→ Room 1	→ Room 2	→ Room 3	Avg
CrossSense	72.78	81.75	82.76	79.09
EI	75.73	84.54	83.98	81.42
Widar 3.0	81.58	93.47	91.08	88.87
Ours	83.93	94.88	92.85	90.55

rooms as the source domains data and the other one as the target domain. The dataset contains 9 persons’ gesture samples in Room 1, 3 persons’ gesture samples in Room 2, and 4 persons’ gesture samples in Room 3, respectively. The results in Table 4 show that we have an overall accuracy of 90.55%, which is the highest average accuracy. Moreover, our framework has an improvement of 0.68% over the Widar 3.0.

(5) *Comparison with CACDGR*: Due to the fact that the CACDGR model [24] only uses very small part of the Widar 3.0 dataset to evaluate their model, we also use the same part of dataset similar with CACDGR to compare our framework with their model. We evaluate the performance on the environment domain. Same as CACDGR, we keep each room’s person number as the same. We choose 3 persons from each room and obtain a subset of the whole dataset which is *User 14 – 16* in Room 1, *User1, User2, User6* in Room 2 and *User 7 – 9* in Room 3. The experiments take one room’s data as the source domains. From Table 5, we find that our framework has the highest accuracy of 88.80%.

TABLE 5: Accuracy (%) Comparison with CACDGR

Methods	Room 1	Room 2	Room 3	Avg
Widar 3.0	87.50	86.36	85.16	86.34
CACDGR	87.30	87.40	88.80	87.83
Ours	89.36	89.10	87.94	88.80

In general, our framework has the highest average accuracy in four domains (locations, orientations, subjects and environments), which shows that our framework indeed improves performance in the unlabeled target domain on Wi-Fi signal dataset.

5.2 Experiment with mmWave Radar Signals

5.2.1 Dataset

We use the public dataset [57], which is collected from 25 volunteers, 6 environments and 5 locations to evaluate our framework. Fig. 4 shows one of the evaluation environments and Fig. 5 illustrates the setup of 5 locations in each environment. The dataset contains six common gestures including push (PH), pull (PL), left swipe (LS) right swipe (RS), clockwise turning (CT) and anticlockwise turning (AT). Each volunteer is asked to perform each kind of gesture 5 times at each location. In total, the dataset has collected 10800 samples.



Fig. 4: Experiment setting with mmWave radar signals.

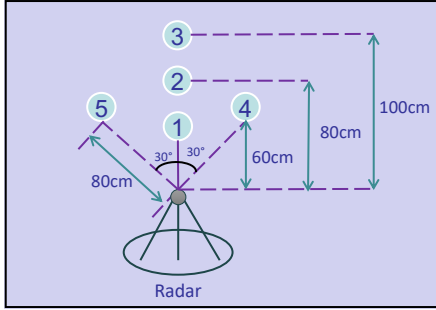


Fig. 5: A typical setup of devices in one environment.

5.2.2 Data Preprocessing

As shown in Fig. 6, To obtain the Dynamic Range Angle Image (DRAI) sequences for gesture recognition, we first employ 3D-FFT on raw signals to derive the ranges, velocities and angles of hands. Then, we adopt noise elimination to filter environmental interference and improve the robustness of the recognition model.

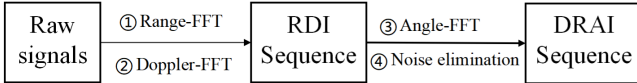


Fig. 6: The calculation process of DRAI sequences.

In specific, the radar continuously transmits FMCW signals and mixes the received chirp to obtain an intermediate frequency (IF) signal. The range of the detected object can be computed using FFT. After that, the radar transmits a frame consisting of N chirps to obtain the velocity of the targeted object. The velocity of the object can be derived from the phase difference caused by the doppler effect between two adjacent chirps. We employ FFT to extract doppler information and obtain Range Doppler Image (RDI). Moreover, the Angle of Arrival (AoA) can be computed by cascading multiple RDIs which are different from each other because there are phase changes between adjacent receiving antennas. The FFT of angle is performed on the direction of receiving antennas to acquire the range-doppler-angle matrix. Finally, we make doppler frequency lower than a velocity threshold as zero to remove static clutter. To obtain the signal intensity of each doppler bin, we sum the averaged range doppler matrix along the range dimension. Only doppler bins whose

signal intensity is higher than the threshold will be counted to obtain DRAI sequences.

5.2.3 Baseline Methods

We compare our approach with two deep learning models RadarNet [27] and Widar3.0 [21]. Specifically, RadarNet designs an efficient neural network and trains a robust model. We first process the mmWave radar signals to Range Doppler Image, then use the Range Doppler Image as the RadarNet model's input. In Widar 3.0 paper, the authors extract the domain invariant feature BVP based on Wi-Fi signals and feed them into a gesture recognition model combining CNN's and GRUs. In this experiment, we use Widar 3.0's gesture recognition model as the backbone model and use the DRAI sequences as the model's input.

5.2.4 Cross Domain Evaluation

We evaluate the performance of the proposed framework on cases crossing different domain factors, including location, subject, and environment. When evaluating on each domain factor, we keep the other domain factors unchanged. For each case, all of the target domain data without labels are used to train with the source data and all the target domain data are used to test. We conduct experiments using all the baseline methods to validate our framework's superiority and generalization ability.

(1) *Cross Location*: To evaluate our framework's performance of crossing location, we use 4 locations of all data as the source domains, and the data of the last location as the target domain. In our experiment, $L1, L2, L3, L4, L5$ represent the five locations of subject. The result comparison is shown in Table 6. Compared to other methods, our framework achieves the highest average accuracy of 95.65% and has significant improvement of 15.23% over the Widar 3.0 and 10.75% over RadarNet. Location L2 has the highest accuracy of 98.84%, which is reasonable since location P2 is the center of other four locations.

TABLE 6: Cross Location Accuracy (%)

Methods	→ L1	→ L2	→ L3	→ L4	→ L5	Avg
RadarNet	67.69	96.81	69.77	95.19	95.05	84.90
Widar 3.0	80.13	97.45	82.59	75.92	65.65	80.32
Ours	91.20	98.84	94.30	96.94	96.95	95.65

(2) *Cross Subject*: Different subjects' data may show different discrepancies due to their various behavior patterns and their body shapes. To evaluate on the impact of different subjects, we use data from $User 1 - 6$ in all rooms to evaluate the model. Each time, we use the data from one user as the target domain and the other users' data as the source domains. The results in Table 7 show our framework achieves the highest average accuracy of 97.97%. All subjects have the accuracy above 93%, $User 1 - 3$ have the accuracy above 99%, which almost 100%. In addition, the average accuracy of our method is 1.52% higher than Widar 3.0.

TABLE 7: Cross Subject Accuracy (%)

Methods	→U1	→U2	→U3	→U4	→U5	→U6	Avg
RadarNet	95.06	92.93	83.06	85.20	90.26	90.40	89.48
Widar 3.0	98.80	98.13	91.85	98.33	98.83	92.78	96.45
Ours	99.42	99.02	93.28	99.33	98.83	96.90	97.97

(3) *Cross Environment*: Different rooms have different layouts, which have an influence on the signal propagation path. To evaluate the impact of the environment, we use the gesture samples collected in five rooms as the source domains data and the one as the target domain. $E 1 - 6$ represent the six environments. The results in Table 8 show that we achieve an overall accuracy of 99.04%, which is the highest average accuracy. All environments have the accuracy above 98%. Moreover, our method has a improvement of 2.25% over the Widar 3.0 and 2.83% over the RadarNet.

TABLE 8: Cross Environment Accuracy (%)

Methods	→E1	→E2	→E3	→E4	→E5	→E6	Avg
RadarNet	99.09	97.11	92.47	98.66	98.00	91.93	96.21
Widar 3.0	97.33	98.53	94.80	95.06	98.13	96.93	96.79
Ours	99.19	98.93	98.66	99.46	98.93	99.06	99.04

In conclusion, similar to the experiment on Wi-Fi signals, our framework achieves considerable improvement of performance in the unlabeled target domain on mmWave radar signal dataset, which shows the superiority of our framework.

5.3 Ablation Study

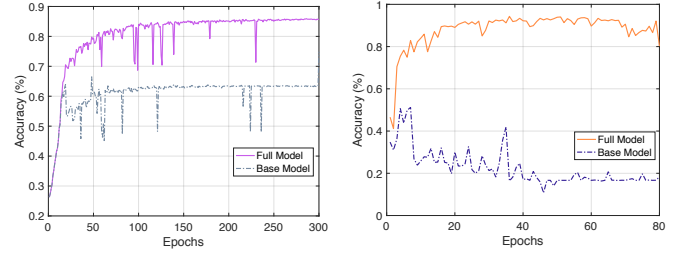
In this section, we perform extensive ablation study on the two RF signals to understand the impact of confidence control constraint, data augmentation methods and pseudo labeling.

5.3.1 Impact of Confidence Control Constraint

In this sub-section, we study the impact of the confidence control constraint, then evaluate the impact of different weights η of confidence control constraint in the final objective. We evaluate the impact of the constraint and different weights with the Wi-Fi signal and mmWave radar signal, respectively. Furthermore, we conduct experiments on five orientation domains with Wi-Fi signal and the five location domains with mmWave radar signal. We use one domain data as the target domain and the remaining domain data as the source domain. We train the model with source domain data and test it on target domain data. The accuracy corresponding to each threshold is the average result of the five target domains.

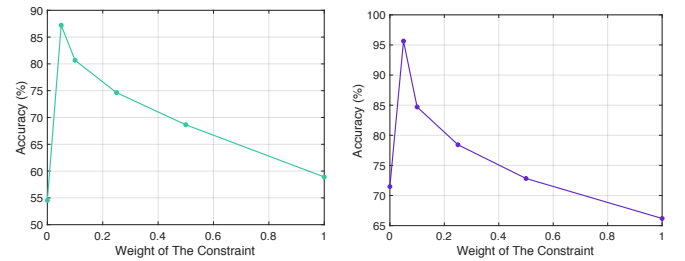
To understand whether the proposed framework always can achieve the effective performance without constraint, we first compare the full model with *base* model (without confidence control constraint). On Wi-Fi dataset, Fig. 7(a) shows that the performance of the model without the confidence control constraint is worse than the performance of the full model. On mmWave radar dataset, Fig. 7(b) shows

that the full model achieves the the accuracy above the 90%, while the base model is difficult to converge. This indicates that the confidence control constraint is necessary and effective for our framework on Wi-Fi dataset and mmWave radar dataset.



(a) Impact of Confidence Control Constraint on Wi-Fi Dataset (b) Impact of Confidence Control Constraint on mmWave Radar Dataset

Fig. 7: Impact of Confidence Control Constraint.



(a) Impact of Constraint's Weight on Wi-Fi Dataset (b) Impact of Constraint's Weight on mmWave Radar Dataset

Fig. 8: Impact of Constraint's Weight.

Then, we employ the analysis experiment to evaluate the impact of different constraint weights η . In specific, we compare the performance of our framework with different constraint weights. The weight values η in this experiment ranges from 0 to 1. From Fig. 8(a), we find that the weight value of 0.92 shows the highest accuracy on Wi-Fi dataset. Fig. 8(b) shows that the model achieve the best performance on mmWave radar dataset when the weight value is 0.95.

5.3.2 Impact of Data Augmentation

To study the impact of the data augmentation methods, we employ experiments with the two RF-based signals: Wi-Fi signal and mmWave radar signal. In specific, we conduct the ablation experiments with five orientations data on Wi-Fi signals and five locations data on mmWave radar signals. We use four domain data as source domains and the remaining domain data as the target domain. We compare the full model with *bare* model (without data augmentation). From Table 9, we can observe that the performance of the model without data augmentation drops 1.25% on Wi-Fi dataset. The Table 10 shows that the the classification accuracy of the base model is not good as the model adopting the data augmentation. Thus, we can summarize that the data augmentation plays important roles in our framework.

TABLE 9: Impact of Data Augmentation with Wi-Fi Signal

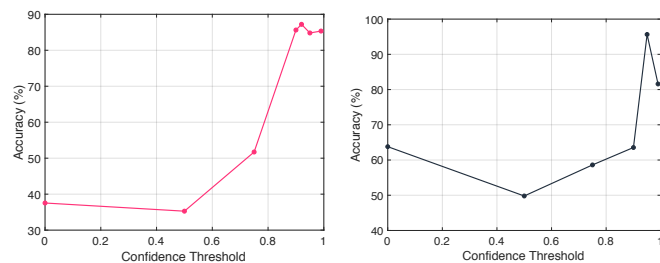
Methods	→ 1	→ 2	→ 3	→ 4	→ 5	Avg
Bare Model	85.66	90.88	90.74	84.94	77.62	85.96
Full Model	87.44	91.64	91.98	85.46	79.53	87.21

TABLE 10: Impact of Data Augmentation with mmWave Radar Signal

Methods	→ 1	→ 2	→ 3	→ 4	→ 5	Avg
Bare Model	90.01	95.30	92.45	93.21	92.37	92.66
Full Model	91.20	98.84	94.30	96.94	96.95	95.65

5.3.3 Impact of Pseudo Label Threshold

In our framework, we use pseudo labeling technique to obtain the pseudo labels of the unlabeled target domain data. The accuracy of the pseudo labeling have a significant impact on the performance of our framework. To reduce the number of incorrect pseudo labels, we utilize the threshold to select the highly confident data. In the subsection, we study the impact of different pseudo label initial threshold. In specific, we employ the analysis on the five location domains with mmWave radar signal and the five orientation domains with Wi-Fi signal. The initial threshold values in this experiment ranges from 0 to 0.99. In the Fig. 9, the accuracy corresponding to each threshold is the average result of the five domains. The Fig. 9(a) shows the impact of the confidence threshold on Wi-Fi dataset. The performance of the recognition model improves with the threshold increasing and achieves the highest accuracy of 91.98% when the initial threshold value is 0.92. The Fig. 9(b) shows that the accuracy of model training with mmWave radar signal drops when using a small initial threshold value and achieves the highest accuracy of 95.65% when the initial threshold value is 0.95.



(a) Impact of Confidence Threshold on Wi-Fi Dataset. (b) Impact of Confidence Threshold on mmWave Radar Dataset.

Fig. 9: Impact of Confidence Threshold.

6 CONCLUSION

In this paper, we propose an unsupervised domain adaptation framework for RF-based gesture recognition. Our framework can increase the capability of cross domain recognition by adopting pseudo-labeling and consistency regularization with elaborated design. Utilizing two data augmentation methods and a confidence control constraint,

our framework achieves state-of-the-art prediction performance. We conduct experiments on two different device-free gesture recognition testbeds, i.e., Wi-Fi and mmWave, to evaluate the performance of the proposed framework. The experimental results demonstrated the superiority of our framework over existing ones. The proposed framework can be extended to other wireless signals, enabling applications in future smart home environments.

REFERENCES

- [1] G. Gkioxari, R. Girshick, P. Dollár, and K. He, "Detecting and recognizing human-object interactions," in *Proceedings of the IEEE Conference on Computer Vision and Pattern Recognition*, 2018, pp. 8359–8367.
- [2] M. Wang, B. Ni, and X. Yang, "Recurrent modeling of interaction context for collective activity recognition," in *Proceedings of the IEEE Conference on Computer Vision and Pattern Recognition*, 2017, pp. 3048–3056.
- [3] A. Bulling, U. Blanke, and B. Schiele, "A tutorial on human activity recognition using body-worn inertial sensors," *ACM Computing Surveys (CSUR)*, vol. 46, no. 3, pp. 1–33, 2014.
- [4] Y. Guan and T. Plötz, "Ensembles of deep lstm learners for activity recognition using wearables," *Proceedings of the ACM on Interactive, Mobile, Wearable and Ubiquitous Technologies*, vol. 1, no. 2, pp. 1–28, 2017.
- [5] X. Huang and M. Dai, "Indoor device-free activity recognition based on radio signal," *IEEE Transactions on Vehicular Technology*, vol. 66, no. 6, pp. 5316–5329, 2016.
- [6] Y. Wang, J. Liu, Y. Chen, M. Gruteser, J. Yang, and H. Liu, "E-eyes: device-free location-oriented activity identification using fine-grained wifi signatures," in *Proceedings of the 20th annual international conference on Mobile computing and networking*, 2014, pp. 617–628.
- [7] S. Shi, S. Sigg, W. Zhao, and Y. Ji, "Monitoring attention using ambient fm radio signals," *IEEE Pervasive Computing*, vol. 13, no. 1, pp. 30–36, 2014.
- [8] W. Wang, A. X. Liu, M. Shahzad, K. Ling, and S. Lu, "Device-free human activity recognition using commercial wifi devices," *IEEE Journal on Selected Areas in Communications*, vol. 35, no. 5, pp. 1118–1131, 2017.
- [9] Y. Ma, G. Zhou, S. Wang, H. Zhao, and W. Jung, "Signfi: Sign language recognition using wifi," *Proceedings of the ACM on Interactive, Mobile, Wearable and Ubiquitous Technologies*, vol. 2, no. 1, pp. 1–21, 2018.
- [10] Y. He, Y. Chen, Y. Hu, and B. Zeng, "Wifi vision: sensing, recognition, and detection with commodity mimo-ofdm wifi," *IEEE Internet of Things Journal*, vol. 7, no. 9, pp. 8296–8317, 2020.
- [11] D. Zhang, Y. Hu, Y. Chen, and B. Zeng, "Breathtrack: Tracking indoor human breath status via commodity wifi," *IEEE Internet of Things Journal*, vol. 6, no. 2, pp. 3899–3911, 2019.
- [12] D. Zhang, Y. He, X. Gong, Y. Hu, Y. Chen, and B. Zeng, "Multitarget aoa estimation using wideband lfm-cw signal and two receiver antennas," *IEEE Transactions on Vehicular Technology*, vol. 67, no. 8, pp. 7101–7112, 2018.
- [13] Y. He, D. Zhang, Y. Hu, and Y. Chen, "Non-line-of-sight imaging with radio signals," in *2020 Asia-Pacific Signal and Information Processing Association Annual Summit and Conference (APSIPA ASC)*. IEEE, 2020, pp. 11–16.
- [14] J. Lien, N. Gillian, M. E. Karagozler, P. Amihoud, C. Schwesig, E. Olson, H. Raja, and I. Poupyrev, "Soli: Ubiquitous gesture sensing with millimeter wave radar," *ACM Transactions on Graphics (TOG)*, vol. 35, no. 4, pp. 1–19, 2016.
- [15] S. Zhu, J. Xu, H. Guo, Q. Liu, S. Wu, and H. Wang, "Indoor human activity recognition based on ambient radar with signal processing and machine learning," in *2018 IEEE international conference on communications (ICC)*. IEEE, 2018, pp. 1–6.
- [16] T. Fan, C. Ma, Z. Gu, Q. Lv, J. Chen, D. Ye, J. Huangfu, Y. Sun, C. Li, and L. Ran, "Wireless hand gesture recognition based on continuous-wave doppler radar sensors," *IEEE Transactions on Microwave Theory and Techniques*, vol. 64, no. 11, pp. 4012–4020, 2016.
- [17] C. L. Li, M. Liu, and Z. Cao, "Wihf: Gesture and user recognition with wifi," *IEEE Transactions on Mobile Computing*, 2020.

- [18] Y. Zou, J. Xiao, J. Han, K. Wu, Y. Li, and L. M. Ni, "Grfid: A device-free rfid-based gesture recognition system," *IEEE Transactions on Mobile Computing*, vol. 16, no. 2, pp. 381–393, 2016.
- [19] H. Abdelnasser, K. Harras, and M. Youssef, "A ubiquitous wifi-based fine-grained gesture recognition system," *IEEE Transactions on Mobile Computing*, vol. 18, no. 11, pp. 2474–2487, 2018.
- [20] A. Virmani and M. Shahzad, "Position and orientation agnostic gesture recognition using wifi," in *Proceedings of the 15th Annual International Conference on Mobile Systems, Applications, and Services*, 2017, pp. 252–264.
- [21] Y. Zheng, Y. Zhang, K. Qian, G. Zhang, Y. Liu, C. Wu, and Z. Yang, "Zero-effort cross-domain gesture recognition with wi-fi," in *Proceedings of the 17th Annual International Conference on Mobile Systems, Applications, and Services*, 2019, pp. 313–325.
- [22] J. Zhang, Z. Tang, M. Li, D. Fang, P. Nurni, and Z. Wang, "Crosssense: Towards cross-site and large-scale wifi sensing," in *Proceedings of the 24th Annual International Conference on Mobile Computing and Networking*, 2018, pp. 305–320.
- [23] W. Jiang, C. Miao, F. Ma, S. Yao, Y. Wang, Y. Yuan, H. Xue, C. Song, X. Ma, D. Koutsonikolas *et al.*, "Towards environment independent device free human activity recognition," in *Proceedings of the 24th Annual International Conference on Mobile Computing and Networking*, 2018, pp. 289–304.
- [24] H. Kang, Q. Zhang, and Q. Huang, "Context-aware wireless based cross domain gesture recognition," *IEEE Internet of Things Journal*, 2021.
- [25] H. Liu, Y. Wang, A. Zhou, H. He, W. Wang, K. Wang, P. Pan, Y. Lu, L. Liu, and H. Ma, "Real-time arm gesture recognition in smart home scenarios via millimeter wave sensing," *Proceedings of the ACM on Interactive, Mobile, Wearable and Ubiquitous Technologies*, vol. 4, no. 4, pp. 1–28, 2020.
- [26] P. S. Santhalingam, A. A. Hosain, D. Zhang, P. Pathak, H. Rangwala, and R. Kushalnagar, "mmasl: Environment-independent asl gesture recognition using 60 ghz millimeter-wave signals," *Proceedings of the ACM on Interactive, Mobile, Wearable and Ubiquitous Technologies*, vol. 4, no. 1, pp. 1–30, 2020.
- [27] E. Hayashi, J. Lien, N. Gillian, L. Giusti, D. Weber, J. Yamanaka, L. Bedal, and I. Poupyrev, "Radarnet: Efficient gesture recognition technique utilizing a miniature radar sensor," in *Proceedings of the 2021 CHI Conference on Human Factors in Computing Systems*, 2021, pp. 1–14.
- [28] X. J. Zhu, "Semi-supervised learning literature survey," 2005.
- [29] M. Sajjadi, M. Javanmardi, and T. Tasdizen, "Regularization with stochastic transformations and perturbations for deep semi-supervised learning," *Advances in neural information processing systems*, vol. 29, pp. 1163–1171, 2016.
- [30] A. Tarvainen and H. Valpola, "Mean teachers are better role models: Weight-averaged consistency targets improve semi-supervised deep learning results," *arXiv preprint arXiv:1703.01780*, 2017.
- [31] K. Sohn, D. Berthelot, C.-L. Li, Z. Zhang, N. Carlini, E. D. Cubuk, A. Kurakin, H. Zhang, and C. Raffel, "Fixmatch: Simplifying semi-supervised learning with consistency and confidence," *arXiv preprint arXiv:2001.07685*, 2020.
- [32] Q. Xie, Z. Dai, E. Hovy, M.-T. Luong, and Q. V. Le, "Unsupervised data augmentation for consistency training," *arXiv preprint arXiv:1904.12848*, 2019.
- [33] D.-H. Lee *et al.*, "Pseudo-label: The simple and efficient semi-supervised learning method for deep neural networks," in *Workshop on challenges in representation learning, ICML*, vol. 3, no. 2, 2013, p. 896.
- [34] S. Ben-David, J. Blitzer, K. Crammer, F. Pereira *et al.*, "Analysis of representations for domain adaptation," *Advances in neural information processing systems*, vol. 19, p. 137, 2007.
- [35] M. Long, Y. Cao, J. Wang, and M. Jordan, "Learning transferable features with deep adaptation networks," in *International conference on machine learning*. PMLR, 2015, pp. 97–105.
- [36] M. Long, H. Zhu, J. Wang, and M. I. Jordan, "Deep transfer learning with joint adaptation networks," in *International conference on machine learning*. PMLR, 2017, pp. 2208–2217.
- [37] G. Kang, L. Jiang, Y. Yang, and A. G. Hauptmann, "Contrastive adaptation network for unsupervised domain adaptation," in *Proceedings of the IEEE/CVF Conference on Computer Vision and Pattern Recognition*, 2019, pp. 4893–4902.
- [38] E. Tzeng, J. Hoffman, K. Saenko, and T. Darrell, "Adversarial discriminative domain adaptation," in *Proceedings of the IEEE conference on computer vision and pattern recognition*, 2017, pp. 7167–7176.
- [39] S. Sankaranarayanan, Y. Balaji, C. D. Castillo, and R. Chellappa, "Generate to adapt: Aligning domains using generative adversarial networks," in *Proceedings of the IEEE Conference on Computer Vision and Pattern Recognition*, 2018, pp. 8503–8512.
- [40] Y. Ganin, E. Ustinova, H. Ajakan, P. Germain, H. Larochelle, F. Laviolette, M. Marchand, and V. Lempitsky, "Domain-adversarial training of neural networks," *The journal of machine learning research*, vol. 17, no. 1, pp. 2096–2030, 2016.
- [41] M.-Y. Liu, T. Breuel, and J. Kautz, "Unsupervised image-to-image translation networks," in *Advances in neural information processing systems*, 2017, pp. 700–708.
- [42] D. Berthelot, N. Carlini, E. D. Cubuk, A. Kurakin, K. Sohn, H. Zhang, and C. Raffel, "Remixmatch: Semi-supervised learning with distribution alignment and augmentation anchoring," *arXiv preprint arXiv:1911.09785*, 2019.
- [43] D. Berthelot, N. Carlini, I. Goodfellow, N. Papernot, A. Oliver, and C. Raffel, "Mixmatch: A holistic approach to semi-supervised learning," *arXiv preprint arXiv:1905.02249*, 2019.
- [44] X. Zhai, A. Oliver, A. Kolesnikov, and L. Beyer, "S4l: Self-supervised semi-supervised learning," in *Proceedings of the IEEE/CVF International Conference on Computer Vision*, 2019, pp. 1476–1485.
- [45] S. Ao, X. Li, and C. Ling, "Fast generalized distillation for semi-supervised domain adaptation," in *Proceedings of the AAAI Conference on Artificial Intelligence*, vol. 31, no. 1, 2017.
- [46] K. Saito, D. Kim, S. Sclaroff, T. Darrell, and K. Saenko, "Semi-supervised domain adaptation via minimax entropy," in *Proceedings of the IEEE/CVF International Conference on Computer Vision*, 2019, pp. 8050–8058.
- [47] C. Qin, L. Wang, Q. Ma, Y. Yin, H. Wang, and Y. Fu, "Contradictory structure learning for semi-supervised domain adaptation," in *Proceedings of the 2021 SIAM International Conference on Data Mining (SDM)*. SIAM, 2021, pp. 576–584.
- [48] D. Li and T. Hospedales, "Online meta-learning for multi-source and semi-supervised domain adaptation," in *European Conference on Computer Vision*. Springer, 2020, pp. 382–403.
- [49] L. Yang, Y. Wang, M. Gao, A. Shrivastava, K. Q. Weinberger, W.-L. Chao, and S.-N. Lim, "Mico: Mixup co-training for semi-supervised domain adaptation," *arXiv e-prints*, pp. arXiv–2007, 2020.
- [50] Y. Chen, H. Deng, D. Zhang, and Y. Hu, "Speednet: Indoor speed estimation with radio signals," *IEEE Internet of Things Journal*, vol. 8, no. 4, pp. 2762–2774, 2020.
- [51] D. Zhang, Y. Hu, Y. Chen, and B. Zeng, "Calibrating phase offsets for commodity wifi," *IEEE Systems Journal*, vol. 14, no. 1, pp. 661–664, 2019.
- [52] Q. Xu, Y. Chen, B. Wang, and K. R. Liu, "Trieds: Wireless events detection through the wall," *IEEE Internet of Things Journal*, vol. 4, no. 3, pp. 723–735, 2017.
- [53] Y. Han, Y. Chen, B. Wang, and K. R. Liu, "Enabling heterogeneous connectivity in internet of things: A time-reversal approach," *IEEE Internet of Things Journal*, vol. 3, no. 6, pp. 1036–1047, 2016.
- [54] D. Zhang, Y. Hu, and Y. Chen, "Mtrack: Tracking multiperson moving trajectories and vital signs with radio signals," *IEEE Internet of Things Journal*, vol. 8, no. 5, pp. 3904–3914, 2020.
- [55] Y. Chen, X. Su, Y. Hu, and B. Zeng, "Residual carrier frequency offset estimation and compensation for commodity wifi," *IEEE Transactions on Mobile Computing*, vol. 19, no. 12, pp. 2891–2902, 2019.
- [56] Z. Wang, S. Chen, W. Yang, and Y. Xu, "Environment-independent wi-fi human activity recognition with adversarial network," in *ICASSP 2021–2021 IEEE International Conference on Acoustics, Speech and Signal Processing (ICASSP)*. IEEE, 2021, pp. 3330–3334.
- [57] Y. Li, D. Zhang, J. Chen, J. Wan, D. Zhang, Y. Hu, Q. Sun, and Y. Chen, "Towards domain-independent and real-time gesture recognition using mmwave signal," *arXiv preprint arXiv:2111.06195*, 2021.
- [58] J. Li, Z. Wang, and X. Hu, "Learning intact features by erasing-inpainting for few-shot classification," in *Proceedings of the AAAI Conference on Artificial Intelligence*, vol. 35, no. 9, 2021, pp. 8401–8409.
- [59] J. Zhang, F. Wu, B. Wei, Q. Zhang, H. Huang, S. W. Shah, and J. Cheng, "Data augmentation and dense- lstm for human activity recognition using wifi signal," *IEEE Internet of Things Journal*, vol. 8, no. 6, pp. 4628–4641, 2020.
- [60] N. Qian, "On the momentum term in gradient descent learning algorithms," *Neural networks*, vol. 12, no. 1, pp. 145–151, 1999.